Journal of NUCLEAR SCIENCE and TECHNOLOGY, Supplement 4, p. 369–372 (March 2004)

Development of a 3-D X-Ray Micro-tomography System and its Application to Trabecular Bone/Cement Interface

Yong Ki CHI and Gyuseong CHO

Department of nuclear and quantum engineering, KAIST, Yu-sung gu, Daejeon, Korea

In recent years, the interface analysis of micro-structure based objects is an important research in osteoporosis, vascular imaging since a 3-D X-ray micro-tomography system was developed. However, the micro-tomographic image shows the white-out appearance in case of imaging of similar density objects with low energy X-ray. Therefore these images must be analyzed about the interface between micro-structure based objects for its application to biomechanical study. Many published studies suggested approximately assumed model of interface and predicted mechanical failure by means of Finite Element Method (FEM) but these FEM analysis has not used for modeling the real structure and interface between objects such as roughness, voids and pores of objects.

We developed micro-tomography system and suggest the application of micro-tomographic image for predicting mechanical failure at the interface. The micro-tomography system consists of a 5 μm micro-focus X-ray tube, a CMOS-based image sensor and a rotating sample holder controlled by a precision motor. CMOS image sensor has 62×62 mm^2 sensing area and uses optical lenses system for increasing resolution. The sample which was manufactured by implanting cement in a pig hip bone was used and its fracture is considered to be an important cause of loosening of hip joint replacement in orthopedic implants. A Feldkamp's cone-beam reconstruction algorithm on the equispatial detector case was used for bone/cement 3D volume data and the analysis of a trabecular bone/cement interface containing white-out appearance was performed by using multiple criterion segmentation of region and volume. Finally, the segmented data can be used for fracture prediction of FEM by determining node of hexahedron meshing.

In this paper, we present development of a 3-D cone beam micro-tomographic system with CMOS image sensor and its application to a complex structure of a trabecular bone and implanted cement for predicting the failure mechanism of orthopedic implants due to stress and pressure. We will also show that how the segmented data is used as geometric input data of I-DEAS for FEM simulation.

KEYWORDS: Trabecular network, bone/cement interface, Micro-CT, Cone-beam CT, FEM

I. Introduction

Since the introduction of computer-based tomographic imaging nearly 30 years ago, advanced diagnostic imaging technologies have revolutionized the practice of medicine [1]. Particularly, the applications of X-ray micro-tomography are various from biomedical to industrial area. [2,3]

The development of high-resolution tomography system has become useful for microstructure-based studies such as cancellous bone, ceramic material and vascular imaging. However, in case of some objects of which dimensions are of the size of detector pixels or of which constructing components have similar densities to each other, segmentation of components in an x-ray tomograph is not easy because the low-contrast nature of objects and the used x-ray photons of low energy made white-out appearance in reconstruction images. One of practical and important examples in bio-studies is the trabecular bone/cement interface of artificial hip joint in orthopedic implants, where the relative density difference between them is within 5% [4].

The analysis of bone/cement interface of artificial hip joint is needed to prevent mechanical failure from rupture and fracture and to determine a particle size, density of cement and an implanting pressure used in orthopedic surgery. Therefore the FEM analysis with a real geometry and property of each bone and cement is promising technique to predict a reliability of orthopedic implants but the existing FEM analysis was related with only trabecular bone or suggested approximately assumed interface model dependent on the property acquired by failure experiments [5,6].

For these analyses, we developed a 3-D X-ray micro-tomographic system with CMOS image sensor which easily makes good use as laboratory equipment because CMOS sensor has the advantages of low power consumption, on-chip integration capability, selective readout, and low cost [7]. The interface between a trabecular bone and cement was separated due to definition of bone/cement property and modeling and of bone/cement structure. As non-isolated bone region is surrounded by cement region and the attenuation coefficient difference of non-isolated bone is smaller than between the difference of void and bone, each region has to be segmented with a multiple criterion method. Edge enhancement and region growing of non-isolated bone region are to divide connected bone/cement and rich cement region is removed with region and volume threshold. Using these criterion methods, radiographically non-distinguished interface is to be apparent.

After segmentation and rendering were done, finally we

Corresponding author: Tel. +82-42-869-3861, Fax. +82-42-869-3810, e-mail: yongkichi@webmail.kaist.ac.kr

visualized 3D elements by using I-DEAS of FEM with micro-tomographic images of bone/cement interface. Currently the analysis of bone/cement interface seems very promising using micro-tomography.

II. Materials and methods

1. System overview

The micro-tomographic system has been arranged in our laboratory. The specification of microfocus X-ray tube is a 9-160 kV high voltage, 0-1mA target current and 5-1000 μm adjustable focal spot. A micro-precision step motor for translating and rotating object is operated under the experiment. An X-ray detector module is based on a CMOS image sensor (**Fig. 1**).

A fine LANEX screen with 4 lp/mm at 30% modulation transfer function(MTF) has been used as the phosphor screen and the sensing area is 62 × 62 mm^2. The CMOS image sensor has 1280 × 1024 pixels, and each pixel size is 9 μmm^2 [8]. The resolution of this detector module is 70 μm and 12 lp/mm could be seen with a standard test pattern using the cone-beam X-ray magnification.

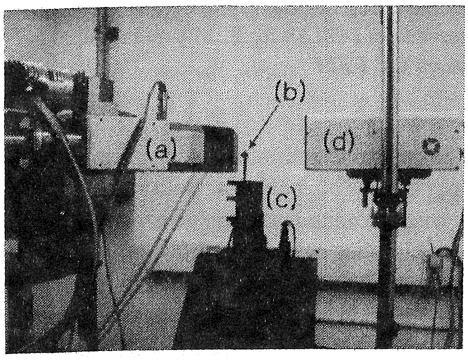

Fig.1 Micro-tomographic system. (a) Microfocus X-ray tube, (b) bone/cement object, (c) micro-precision step motor and (d) CMOS X-ray detector. Fine focus cone-beam X-ray penetrates the object and the transmitted X-ray arrives at CMOS detector which converts it to the signal.

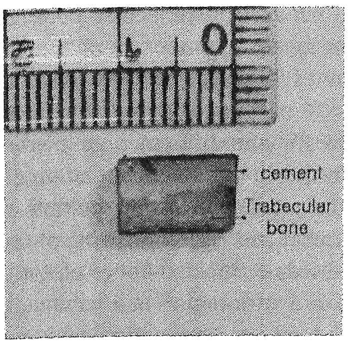

Fig.2 The sample is made of a pig hip bone and cement.

The sample of $10 \times 5 \times 5mm^3$ rough size is composed of a pig hip bone and cement. Uniform air pressure machine implanted cement to a pig hip bone and the bone/cement is cut by diamond cutter in its size (**figure 2**).

The system is mounted on an optical table for isolation of vibration and is installed in a well-shielded room. The control of the X-ray tube, object manipulation, data acquisition, and image processing are done in the control room. All the systems are controlled by a PC.

2. Image Correction and Reconstruction

Scanner motion, detector, data acquisition are controlled through graphical user interface on a Windows-based PC. After PCI (Peripheral Component Interconnect) transfers image data to PC and images are stored, the reconstruction and image processing were carried out with projection data (1280×1024 projection images, 250 projections and 0.072 degree/slice) in PC (**Fig. 3**).

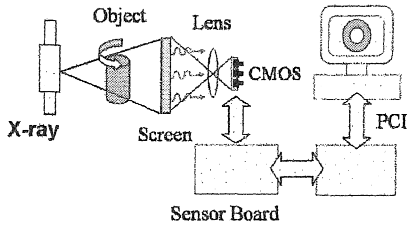

Fig.3 Schematic diagram of micro-tomographic system.

The projection data is acquired by cone-beam X-ray which has a high signal-to-noise ratio and fast scan time of one slice in the 2-D case. A Feldkamp's 3-D cone-beam reconstruction in equispatial detector case was used and the formulation is given by

$$g(x,y,z)=\frac{1}{2}\int_0^{2\pi}\frac{\rho^2(\beta)}{[\rho(\beta)-s]^2}\int_{-\infty}^{\infty}R(p,\varsigma,\beta)\ \times$$
$$f[\frac{\rho(\beta)t}{\rho(\beta)-s}-p]\frac{\rho(\beta)}{\sqrt{\rho^2(\beta)+p^2+\varsigma^2}}dpd\beta$$

where $g(x,y,z)$ is the reconstruction image, $\rho(\beta)$ is the distance from the X-ray source to z axis of the reconstruction system, $R(p,\varsigma,\beta)$ cone-beam projection data as a function of the detector spatial position (p,ς) and the X-ray source angle β, f the reconstruction filter(Shepp-Logan filter).

Reconstruction image has 500 × 500 × 300 voxel data and is reconstructed using a bilinear interpolation. A one dimensional Butter-worth low-pass filter is used for removing the ring artifact. Its transfer function is given by

$$H(u,v) = \begin{cases} \dfrac{1}{1+(\frac{u}{u_0})^{2n}} & if\ |v| \le v_0 \\ 1 & otherwise \end{cases}$$

1-D low pass filtering with the horizontal cutoff frequency u_0 and the filter order n was performed. The other image processing is explained at next stage of 3D visualization.

3. Multiple criterion method

As the reconstructed trabecular bone/cement value is continuous and its image is the white-out appearance, single threshold value is not proper for the segmentation of each bone/cement. Therefore we used a multiple criterion method that makes each region separated with each volume and region criterion of bone/cement.

For the segmentation of bone/cement, two regions have to be solved. First partial cement has the larger value than that of trabecular bone due to pressurized cement but the region of pressurized cement is small circular region and spherical volume. Second non-isolated bone region surrounded by cement has continuous gray value in interface and specific threshold value does not exist due to fluctuation of cement gray value. However, as the edge of non-isolated bone region is forced to be enhanced, it can be segmented by region growing and region criterion. Therefore we are able to finally refine each bone and cement boundary with morphological image operation. These morphological image processing are given by flow diagram (**figure.4**). We obtained the bone/cement region and interface with the above image processing.

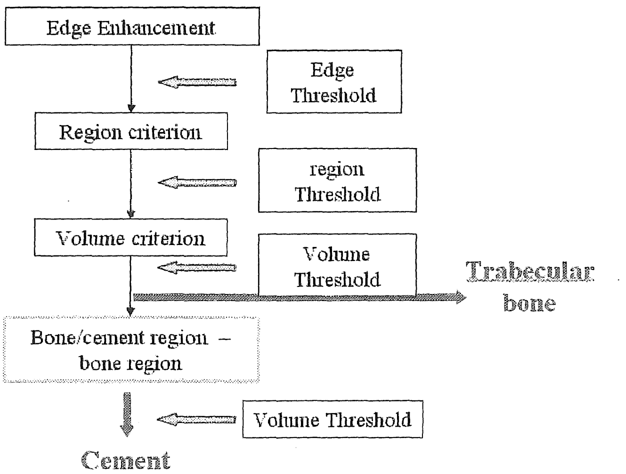

Fig.4 Flow diagram of bone segmentation illustrating overall methods. Region/volume criterion can remove pressured cement region and edge enhancement/region growing can segment non-isolated bone. Isolated bone is easy to be segment by a gray value threshold.

III. Results

1. 3-D Reconstruction

Projection images acquired by CMOS image sensor is gray scale and integrated X-ray intensity for the exposure time. Therefore it has to be converted to an attenuation coefficient value. Entire noise on CMOS sensor was calibrated by subtraction of dark current and gain correction of each pixel (**Fig 5**). These corrections have a good influence upon a ring artifact for the reason that pixel gain and dark current will be uniform for acquiring projection data.

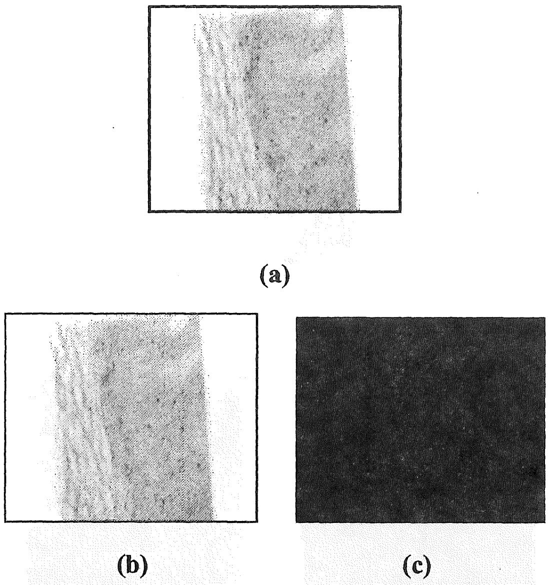

Fig.5 2D projection image (70 keV, 0.5mA). **(a)** original image, **(b)** correction image for dark current and gain of each pixel and **(c)** projection image converted to attenuation coefficient value.

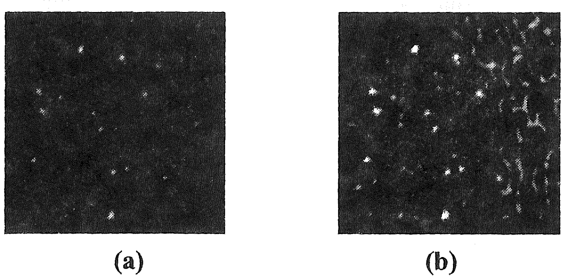

Fig.6 Reconstructed slice image by butterworth and Shepp-Logan filters. **(a)** Bilinear interpolated reconstruction image and **(b)**Removing high frequency and rescaling.

After the noise of gain and dark is removed, ring artifact and high frequency is removed by butter-worth filter and Shepp-logan filters. Backprojection methods are generalized Cone-beam reconstruction in equispatial detector case and bilinear interpolation (**Fig 6**).

Reconstructed slice image cannot distinguish bone and cement using above images but segmented image by minimum gray value threshold has a rough geometry as compared with SEM image (**Fig 7**).

2. Segmentation using Multiple Criterion Method

After the multiple criterion method was applied to the bone/cement, a real geometry such as roughness, voids and pores of objects is obtained (**Fig 8**). The criterions in micro-tomographic images iteratively have to select but it is not difficult due to constant attenuation coefficient of bone/cement and resolution of reconstruction image.

Hexahedron meshing method is applied for determination of node. This method employs a straightforward voxel conversion. Voxels with a gray scale value beyond a segmented threshold value are converted to brick elements in FEM

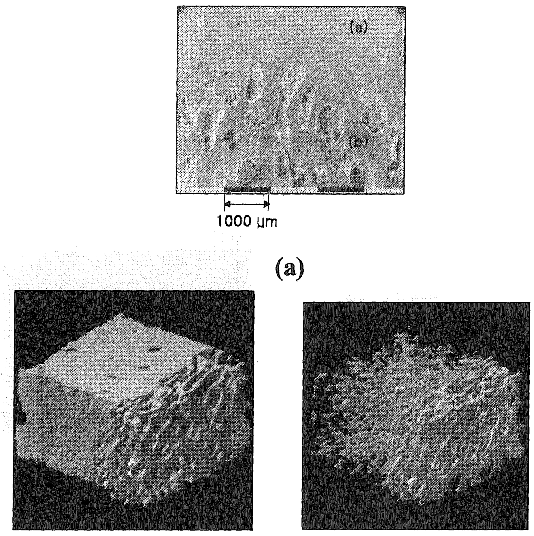

(a)

(b) (c)

Fig.7 Visualization of segmented bone/cement using Iterative Data Language (IDL). **(a)** SEM photography, **(b)** whole bone/cement rendered volume and **(c)** rendered volume by gray level threshold of proper bone value. (b), (c) means that only gray level threshold cannot segment bone region due to rich cement and non-exact difference between trabecular bone and cement. (a) whole bone/cement rendered volume, (b) rendered bone volume by gray level threshold of bone value.

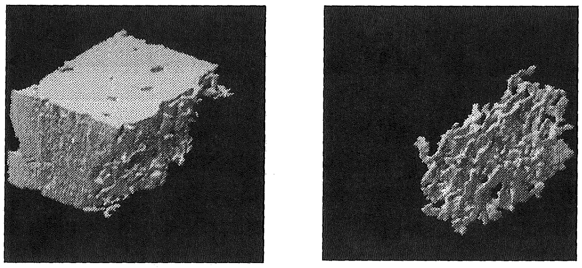

(a) (b)

Fig.8 segmentation by multiple criterion method. **(a)** cement volume and **(b)** trabecular bone volume.

3. Microstructure Analysis for FEM

A 3-D image with the real geometry and property of each material was generated using I-DEAS analysis for FEM simulation (**Fig 9**). Therefore FEM simulation will easily be able to be done with real geometry and property for predicting biomechanical failure such as fracture and rupture.

Acknowledgement

This work is partially supported by Innovative Technology Center for Radiation Safety (iTRS).

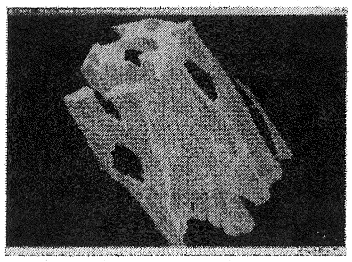

Fig.9 3-D finite element modeling using I-DEAS for ABACUS input file (the partial region of trabecular bone).

IV. Discussion and Conclusion

The analysis of bone/cement interface using micro-tomography is successful and the white-out appearance of bone/cement micro-tomographic image was segmented by the morphological image processing with multiple criterion method. We think that the application for FEM will be helpful to simulate mechanical failure using the real geometry of bone/cement. We expect that reliability-based optimal design of cement in orthopedic implants will be accomplished not by mechanical failure test but by FEM using micro-tomography. Further studies for FEM simulations and failure experiments will be performed for comparing fracture and rupture between simulated and experimental results.

References

1) Hounsfield GN, "Computerized transcerse axial scanning (tomography) : 1. Description of system". Br J Radiol 46, 1016-1022
2) David W. Holdsworth, "Micro-CT in small animal and specimen imaging", Trends in Biotechnology Vol. 20 No. 8, 2002
3) R. Cesareo, "Tomography and Microtomography for Examination of Ceramic Matrials", The e-journal of nondestructive testing Vol.3 No.8, 1998
4) Churchill, "High bone cement pressurization is achieved during femoral stem insertion into viscous cement.", Orthopaedic Research Society, 46th annual meeting, 2000
5) Glen L. Niebur, "High-resolution finite element models with tissue strength asymmetry accurately predict failure of trabecular bone", Journal of Biomechanics, Vol. 33, 1575-1583, 2000.
6) Graham J., "Trabecular orientation, bone porosity and cement pressure significantly affect fracture toughness at the trabecular bone/cement interface", 47th annual meeting, orthopedic research society, February 25-28, 2001
7) S. T. Smith, D. R. Bednarek, D. C. Wobschall, M. Jeong, H. Kim, and S. Rudin, "Evaluation of a CMOS image detector for low cost and power; Medical x-ray imaging applications", Proc. SPIE, Vol. 3659, pp.952-961, 1999.
8) TRADIX 100 Model, Star V-ray, http://www..starvray.com, Korea